Available online at www.sciencedirect.com

ScienceDirect

Procedia Structural Integrity 2 (2016) 2190–2197

Structural Integrity Procedia

www.elsevier.com/locate/procedia

21st European Conference on Fracture, ECF21, 20-24 June 2016, Catania, Italy

Modeling the lifetime reduction due to the superposition of TMF and HCF loadings in cast iron alloys

B. Fedelich[a]*, H.-J. Kühn[a], B. Rehmer[a], B. Skrotzki[a]

[a]*Federal Institute for Materials Research and Testing, Division 5.2, Unter den Eichen, 12205, Berlin, Germany*

Abstract

The superposition of small amplitude, high frequency loading cycles (HCF) to slow, large amplitude loading cycles (TMF) can significantly reduce the fatigue life. In this work, the combined TMF+HCF loading has been experimentally investigated for a cast iron alloy. In particular, the influence of the HCF frequency of the HCF amplitude and of the location of the superposed HCF cycles has been assessed. It was observed that the HCF frequency has a limited impact on the TMF fatigue life. On the other side, the HCF-strain amplitude has a highly non-linear influence on the TMF fatigue life. A simple estimate for the fatigue life reduction due to the superposed HCF cycles has been derived from fracture mechanics considerations. It is assumed that the number of propagation cycles up to failure can be neglected after a threshold for the HCF loading has been reached. The model contains only two adjustable parameters and can be combined with any TMF life prediction model. The model predictions are compared with the test results for a large range of TMF+HCF loading conditions.

Peer-review under responsibility of the Scientific Committee of PCF 2016.

Keywords: Thermomechanical Fatigue (TMF); High Cycle Fatigue (HCF); Cast iron; Fatigue assessment

1. Introduction

Components in combustion engines usually undergo complex thermomechanical low frequent cyclic loadings (Thermo Mechanical Fatigue, TMF) due to start-up and shut-down of the engines. However, high frequency vibrations (High Cycle Fatigue loading, HCF) are often superposed to the basic TMF cycles. In a series of recent papers (see, e.g. Moalla et al., 2001; Beck et al., 2007, 2008 and 2010) it has been shown that this additional loading can dramatically lessen the fatigue life, when expressed in terms of the number of TMF+HCF loading blocks. While

* Corresponding author. Tel.: +49 30 8104 3104; fax: +49 30 8104 1527.
E-mail address: bernard.fedelich@bam.de

Peer review under responsibility of the Scientific Committee of PCF 2016.
10.1016/j.prostr.2016.06.274

the prediction of the fatigue life under TMF loading is still a research area, there is a need for an estimate of the lifetime reduction due to the superposed HCF loading, notwithstanding the tool applied for the pure TMF life prediction. The objective of the present work is to present a simple estimate for this lifetime reduction. It is based on a number of observations that have been made in (Nicholas, 2006; Beck et al., 2007 and 2010; Schweizer et al., 2011; Metzger et al., 2013):

- The fatigue cracks initiate very readily so that the overall fatigue life corresponds to the growth of mechanically short cracks from a few μm up to a few mm.
- The crack initiation is mostly triggered by the TMF loading.
- The crack propagation is controlled by the crack tip plasticity as expressed by the cyclic Crack Tip Opening Displacement $\Delta CTOD$.
- There is a threshold for the effectivity of the HCF vibrations. When this threshold has been reached, a strong acceleration of crack propagation is observed. Below this threshold, the crack growth follows the rate for the TMF loading alone.

Note that the last assumption corresponds to the behavior type A as considered by Nicholas (2006). It is consistent with the crack growth curves presented by Metzger et al. (2013) for cast iron materials.

The present paper first summarizes the results of a series of TMF+HCF combined tests on a ferritic cast iron alloy containing spheroidal graphite nodules. Then a rule to estimate the lifetime reduction due to the superposed HCF vibrations is derived from fracture mechanics based considerations.

2. TMF+HCF Testing

TMF tests with and without superposed HCF loading have been carried out for the ferritic cast iron EN GJS XSiMo 4.05 with spheroidal graphite nodules. The tests focused on 180° out of phase loading, since this represents the typical cycle for heating of a component under constrained strain condition. Furthermore, this represents the most damaging loading case for the surveyed material. The number of cycles to failure was defined at 20 % load drop in the tensile regime. TMF tests were carried out with temperature rates of 5 K/s using variations of temperature in the scope from 300 to 800 °C. The loading was imposed with a strain ratio of $R = \varepsilon_{\min} / \varepsilon_{\max} = -1$ and hold times of 180 s at maximum temperature and $\varepsilon = \varepsilon_{\min}$.

More than fifty tests with superposed HCF vibrations have been performed. The total strain is decomposed in a thermal and a mechanical strain, $\varepsilon_{tot} = \varepsilon_{th} + \varepsilon_m$. The mechanical strain is then the superposition of the slowly varying TMF strain ε_m^{TMF} and the fast oscillating HCF strain ε_m^{HCF}, i.e. $\varepsilon_m = \varepsilon_m^{TMF} + \varepsilon_m^{HCF}$. Note that ε_m^{TMF} can be regarded as a gliding average of the total mechanical strain ε_m. A comprehensive presentation of the results can be found in the final project report by Skrotzki et al. (2015). The effects of the amplitude of the basic TMF test, of the amplitude and the frequency of the HCF have been examined. Fig. 1 shows the variations of the strain components and of the temperature during the various types of tests. In particular, the following combinations of the TMF and the HCF loadings have been carried out:

a) The HCF loading is applied throughout the cycle (Fig. 1a).
b) The HCF loading is only applied during the high temperature compression dwell (Fig. 1b).
c) The HCF loading is applied throughout the cycle, whereas an additional dwell under tension at minimal temperature has been added (Fig. 1c).
d) The HCF loading is only applied at maximal tensile strain $\varepsilon_{m,\max}$ (corresponding to $T_{\min}$) and thus to the maximal tensile stress (Fig. 1d).

In the following, the subscript m for the mechanical strains will be dropped to simplify the notations $(\varepsilon_m = \varepsilon)$.

The Fig. 2a and 2b show some examples of the test results in the case of the TMF strain amplitude of 0.12 %. The temperature range is 300-700 °C. First it can be observed in Fig. 2a that an increase of the HCF frequency from 5 Hz to 20 Hz has almost no impact on the fatigue life, when expressed in terms of the TMF blocks, although it corresponds to four times more HCF loading cycles per TMF block. A single test performed at 1 Hz showed also no significant difference with the other tests at the same HCF amplitude. In Fig. 2a, the presented results concern the

loading type a (HCF vibrations superposed throughout the cycle). This limited dependence on the HCF frequency was observed on almost all test conditions.

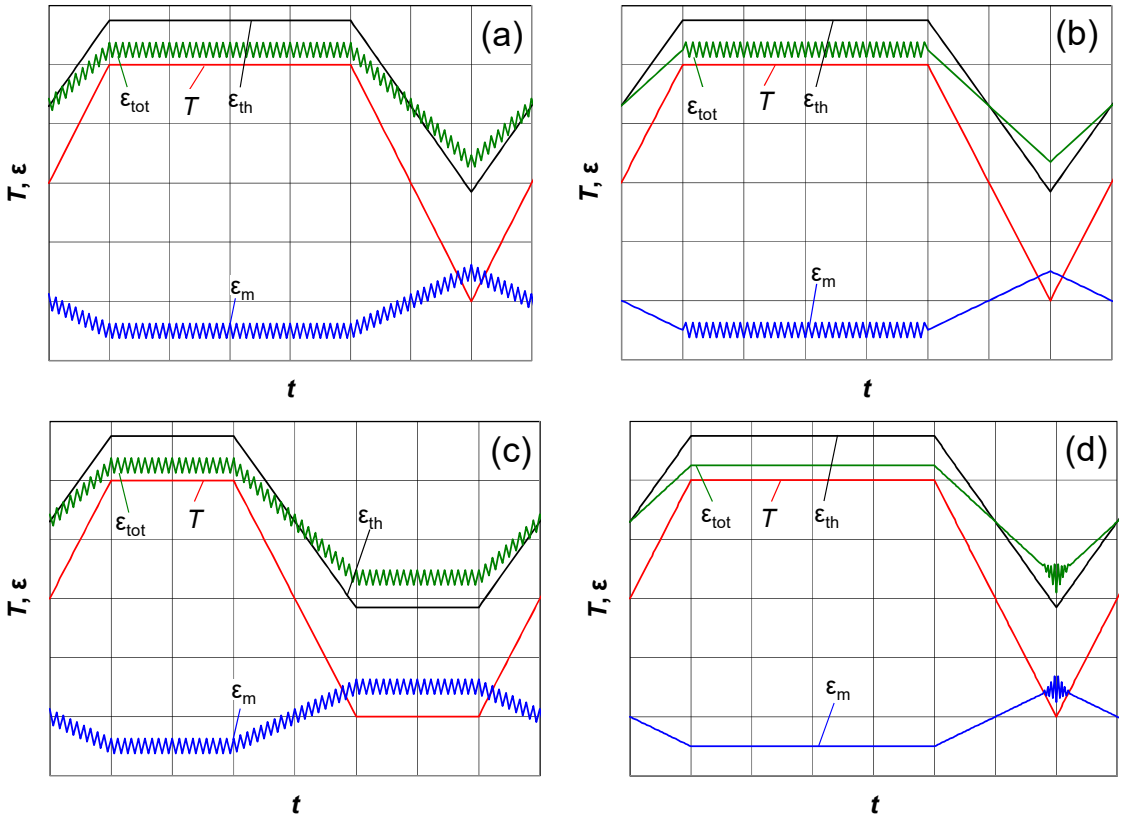

Fig. 1. Schematics of the TMF+HCF loading blocks.

Fig. 2b shows the influence of the TMF+HCF loading combination. At low HCF strain amplitudes, HCF loading during the compression dwell only ("comp dwell", see Fig. 1b) is less detrimental than during the whole cycle ("whole cycle", see Fig. 1a). At the highest amplitude, the difference between both types of loadings is reduced. Note that similar results were reported by Beck et al. (2008) for the cylinder head alloy AlSi6Cu4. Surprisingly, the superposition of HCF vibrations throughout the TMF cycle extended by a dwell under maximal (positive) TMF strain ("tens. dwell", see Fig. 1c) has no damaging effect. However, the superposition of a few HCF vibrations at the TMF peak strain ("max. strain", see Fig. 1d) already noticeably reduces the fatigue life at large HCF strain amplitude, even though not as much as when applied throughout the TMF cycle.

Fig. 3 summarizes the TMF+HCF test results in terms of the fatigue life reduction factor $N^{TMF+HCF} / N^{TMF}$ i.e., the fatigue life for the TMF+HCF loading divided by the fatigue life for the base TMF loading. It includes tests with different temperature ranges and loading types. Note that the tests with identical conditions but different HCF frequencies are represented by the same symbols, since the influence of the HCF frequency is negligible. Also the tests with loading type c are represented together with the tests with loading type a for the same reason.

Beside the types of tests already described, the data includes isothermal LCF+HCF tests with hold time in both tension and compression. In turn, the HCF vibrations are applied either only in tension ("tens. dwell") or only during the compression dwells ("comp. dwell"). The comparison shows that as expected, the superposed HCF loading is more damaging when applied under tension than under compression. Also two tests with a small number of HCF vibrations at the beginning of the compressive dwell ("min. strain") were carried out. The life time reduction is comparable to the superposition of the vibrations throughout the dwell. Finally, a limited number of tests with a 90°

phase shift were performed. The HCF vibrations, which were only superposed during the hold time at maximal temperature ($\varepsilon^{TMF} = 0$), had no detrimental effect. All in all, the test results show a moderate influence of the mean stress at which the HCF vibrations are applied.

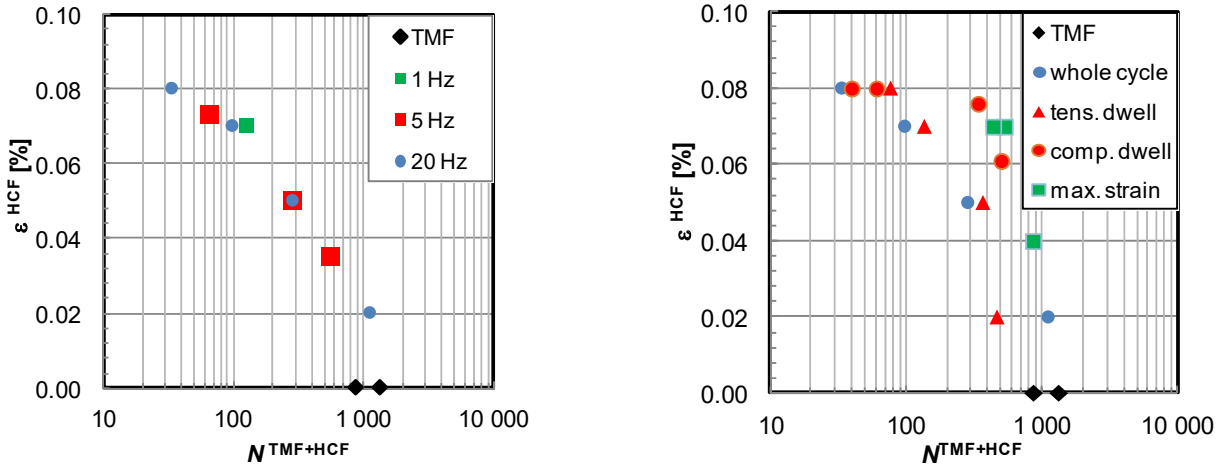

Fig. 2. (a) Influence of the HCF strain amplitude and of the HCF frequency (loading type a); (b) Influence of the loading type at 20 Hz.

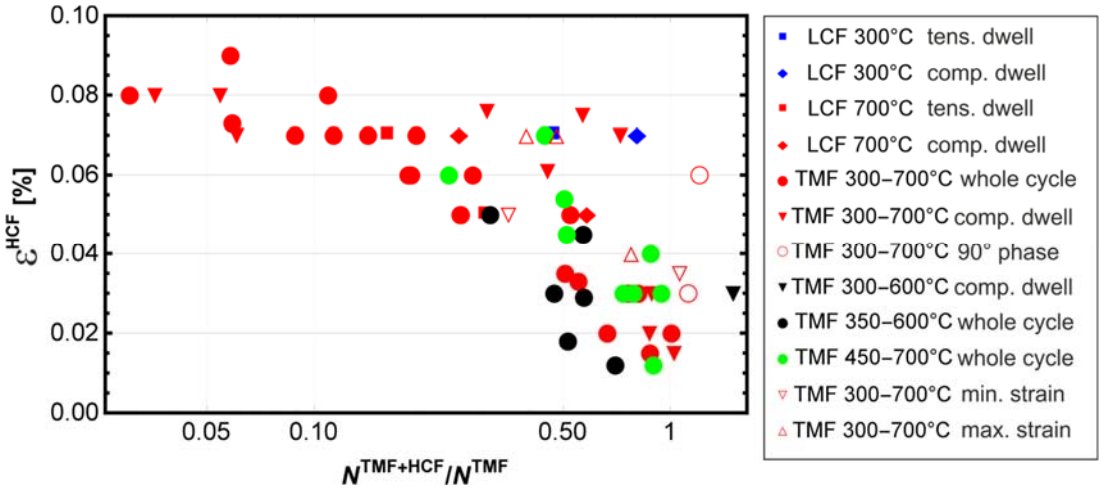

Fig. 3. Fatigue life reduction factor for all TMF+HCF tests. “whole cycle” corresponds to loading type a, “comp. dwell” to loading type b.

3. Estimation of the fatigue life reduction

The experimental results show that the influence of the HCF frequency f^{HCF} is very limited. Hence, damage models based on a linear damage accumulation rule are expected to fail. As an illustration, a HCF loading that halves the fatigue life (from 5000 cycles to 2500 cycles) with a linear summation rule is first considered. Multiplying the number of HCF vibrations by a factor of four, i.e. increasing the frequency from 5 Hz to 20 Hz lessens the number of TMF cycles to failure down to 1000 cycles, which is 1/5th of the pure TMF loading (see Fig. 4a). Such an influence of the HCF frequency was not observed experimentally. With a crack propagation based model, the dependence on the frequency is significantly reduced. Indeed, the total crack growth rate per TMF+HCF block is (see e.g., Hawkyard et al., 1996; Nicholas, 2006)

$$\left.\frac{da}{dn}\right|_{TMF+HCF} = \left.\frac{da}{dn}\right|_{TMF} + \sum_{HCF\ Cycles} \left.\frac{da}{dn}\right|_{HCF} \tag{1}$$

For short cracks, the cyclic Crack Tip Opening Displacement ($\Delta CTOD$) is proportional to the crack depth a. Assuming that the crack growth rate is proportional to $\Delta CTOD$ leads to the formal relationship

$$\left.\frac{da}{dn}\right|_{TMF} = A\,a \tag{2}$$

for the pure TMF loading, where A is a loading dependent constant. Following the ideas of Schweizer et al. (2011) and Metzger et al. (2013), we also consider that the HCF loading is only effective once a critical value $\Delta CTOD_{th}$ is reached, corresponding to some critical crack depth a_{th}. One can then formally rewrite (1) as

$$\left.\frac{da}{dn}\right|_{TMF+HCF} = \begin{cases} A\,a, & a \le a_{th}, \\ A\,a + f^{HCF}\,B\,A\,a, & a > a_{th}, \end{cases} \tag{3}$$

where B is a constant that depends on the magnitude of HCF loading. For the sake of comparison, we assume $a_f = 100\,a_0$, where a_0 is the initial crack depth and a_f the crack depth at failure, $a_{th} = 5\,a_0$ and $f_0^{HCF} B = 3$. With these values, the superposed HCF loading also approximately halves the fatigue life. Increasing the HCF frequency by a factor 4, $f^{HCF} = 4 \times f_0^{HCF}$, now only further reduces the fatigue life down to 2000 TMF blocks instead of 1000 in the case of the linear accumulation rule. The graphic comparison between both types of damage accumulation can be seen in Fig. 4a and b. If a threshold for the HCF loadings exists, the influence of the HCF frequency is significantly reduced due to the strong acceleration of crack growth after exceeding the threshold.

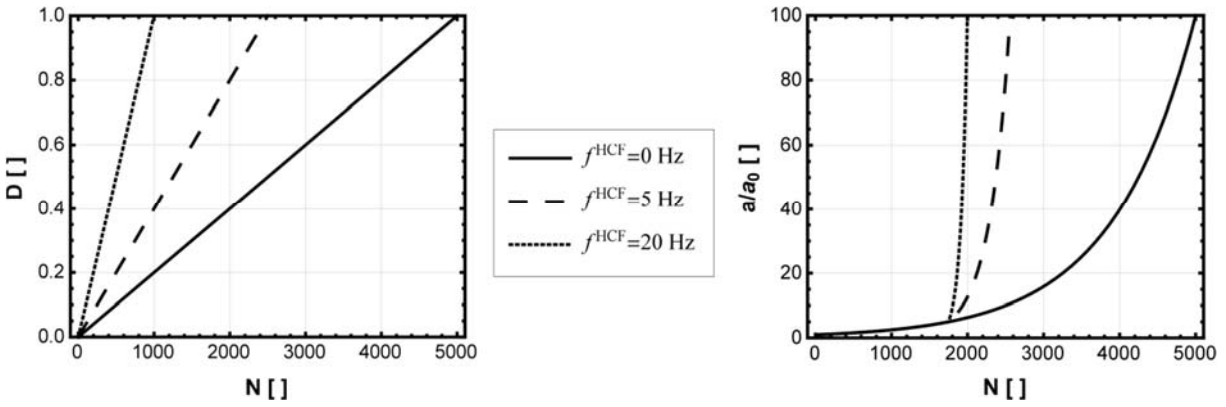

Fig. 4. (a) Linear damage accumulation vs. (b) crack propagation according to equ. (3).

In accordance with the previous considerations, we henceforth assume that the threshold for the HCF vibrations controls the overall fatigue life, i.e. the TMF+HCF blocks beyond the threshold are simply neglected. With this simplification, the pure TMF and the TMF+HCF fatigue lifes follows from equ. (2):

$$\mathrm{Log}\left(\frac{a_f}{a_0}\right) = A\,N^{TMF}, \quad \mathrm{Log}\left(\frac{a_{th}}{a_0}\right) = A\,N^{TMF+HCF}. \tag{4}$$

Thus the fatigue life is simply given by the number of TMF cycles to attain the HCF-threshold. An estimate for the cyclic *CTOD* due to the HCF vibrations is (see e.g. Riedel, 1987)

$$\Delta CTOD^{HCF} = d_{n'} \frac{\left(\Delta\sigma_{eff}^{HCF}\right)^2 \pi a Y^2}{E\,\sigma_{cyc}}, \tag{5}$$

where $\Delta\sigma_{eff}^{HCF}$ denotes the effective stress range, that is the range of the stress in excess of the opening stress σ_{op}. The cyclic yield stress is denoted by σ_{cyc}, $d_{n'}$ is a function of the cyclic hardening exponent n' (see Shih, 1981), Y is a geometric factor and E the Young's modulus. It is assumed that the HCF loading becomes only effective when $\Delta CTOD^{HCF}$ overruns the threshold $\Delta CTOD_{th}$. The critical crack depth can be expressed as function of this threshold as

$$a_{th} = \frac{1}{d_{n'}\pi} \frac{E\,\sigma_{cyc}\,\Delta CTOD_{th}}{\left(Y\,\Delta\sigma_{eff}^{HCF}\right)^2}. \tag{6}$$

Since the temperature and the effective stress range can change during the cycle, the value $\Delta CTOD^{HCF}$ can also change during a TMF block. The maximal value attained by $\Delta CTOD^{HCF}$ during a TMF+HCF block is regarded as being critical for the impact of the HCF vibrations. Thus we consider

$$\underset{HCF\ Cycles}{\mathrm{Sup}}\ \Delta CTOD^{HCF} = \pi a Y^2 \underset{HCF\ Cycles}{\mathrm{Sup}}\ d_{n'} \frac{\left(\Delta\sigma_{eff}^{HCF}\right)^2}{E\,\sigma_{cyc}} = a\,\delta_{eff}^{HCF}, \tag{7}$$

where

$$\delta_{eff}^{HCF} = \underset{HCF\ Cycles}{\mathrm{Sup}}\ \pi Y^2 d_{n'} \frac{\left(\Delta\sigma_{eff}^{HCF}\right)^2}{E\,\sigma_{cyc}}. \tag{8}$$

From equ. (4) to (8) finally result the following estimate for the lifetime reduction $N^{TMF+HCF}/N^{TMF}$ factor:

$$\begin{aligned}
&\text{If } \delta_{eff}^{HCF} \le \frac{\Delta CTOD_{th}}{a_f}, \quad \frac{N^{TMF+HCF}}{N^{TMF}} = 1, \\
&\text{If } \frac{\Delta CTOD_{th}}{a_f} < \delta_{eff}^{HCF} < \frac{\Delta CTOD_{th}}{a_0}, \quad \frac{N^{TMF+HCF}}{N^{TMF}} = \frac{\mathrm{Log}\left(\dfrac{\Delta CTOD_{th}}{a_0\,\delta_{eff}^{HCF}}\right)}{\mathrm{Log}\left(\dfrac{a_f}{a_0}\right)}, \\
&\text{If } \delta_{eff}^{HCF} \ge \frac{\Delta CTOD_{th}}{a_0}, \quad \frac{N^{TMF+HCF}}{N^{TMF}} = 0.
\end{aligned} \tag{9}$$

In the present work, various solutions for the crack opening stress σ_{op} have been tested. It was found that taking the whole stress range i.e. $\Delta\sigma_{eff}^{HCF} = \Delta\sigma^{HCF}$ yielded the best results in terms of the correlation $\left(\delta_{eff}^{HCF}, N^{TMF+HCF}/N^{TMF}\right)$. In other words, we set

$$\delta_{eff}^{HCF} = \delta^{HCF} = \underset{HCF\ Cycles}{\mathrm{Sup}}\ \pi Y^2 d_{n'} \frac{\left(\Delta\sigma^{HCF}\right)^2}{E\,\sigma_{cyc}}, \quad \Delta\sigma^{HCF} = \sigma_{\max}^{HCF} - \sigma_{\min}^{HCF}. \tag{10}$$

The formula (10) has been evaluated for the alloy EN GJS XSiMo 4.05. For this purpose, the parameters σ_{cyc} and n' of the cyclic Ramberg-Osgood model have been determined in the temperature interval 300-700°C. Fig. 5 shows the correlation between δ^{HCF} and the fatigue life reduction factor $N^{TMF+HCF}/N^{TMF}$. Note that the parameter δ^{HCF} is related to the maximal value of $\Delta CTOD^{HCF}$ during a TMF+HCF block by equ. (7). The denominations of the tests are the same as in Fig. 3. Apart from the large scatter, a consistent trend can be observed with no pronounced systematic deviations.

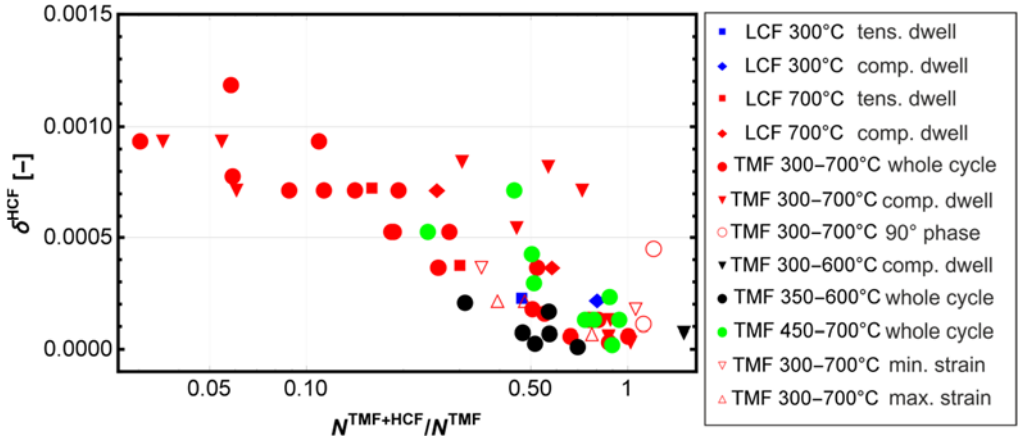

Fig. 5. Correlation between δ^{HCF} and $N^{TMF+HCF}/N^{TMF}$.

Finally, the parameters $\Delta CTOD_{th}/a_0$ and a_f/a_0 needed to evaluate equ. (9) have been determined by fitting the available experimental data. Fig. 6 shows the agreement between the calculated and the experimental fatigue life reduction factors $N^{TMF+HCF}/N^{TMF}$. Despite the simplicity of the model and the fact that only two parameters were fitted, most data points lay within a scatter band of width corresponding to a deviation of a factor 2.

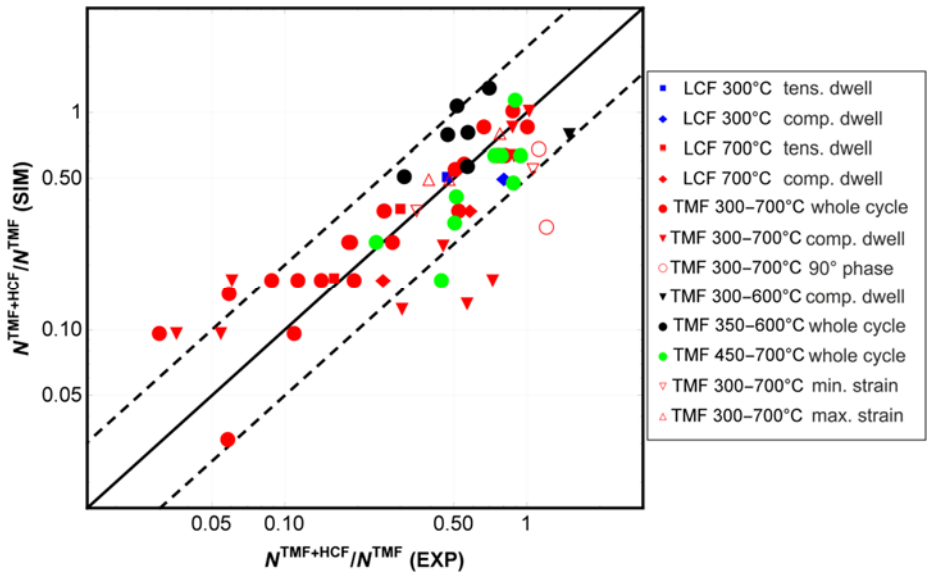

Fig. 6. Predicted lifetime reduction $N^{TMF+HCF}/N^{TMF}$ (SIM) versus experimental lifetime reduction $N^{TMF+HCF}/N^{TMF}$ (EXP).

Acknowledgements

The authors express their thanks to the Research Association for Combustion Engines (FVV, Frankfurt) for the selection of this research project (No. 1100) as well as to the Federal Ministry of Economics and Technology (BMWi) for financial support via the German Federation of Industrial Research Associations (AiF). The project was supervised by an accompanying board of the FVV under the leadership of Dr. H. Haase. Special thanks of the authors go to this board for its wide support.

References

Beck, T., Löhe, D., Luft, J., Henne, I., 2007. Damage mechanisms of cast Al–Si–Mg alloys under superimposed thermal–mechanical fatigue and high-cycle fatigue loading. Materials Science and Engineering A 468–470, 184–192.

Beck, T., Henne, I., Löhe, D., 2008. Lifetime of cast AlSi6Cu4 under superimposed thermal–mechanical fatigue and high-cycle fatigue loading. Materials Science and Engineering A 483–484, 382–386.

Beck, T., Lang, K.-H., Löhe, D., 2010. Interaction of thermally induced and mechanical fatigue. Transactions of The Indian Institute of Metals 63, 195-202.

Skrotzki, B., Uckert, D., Matzak, K., Kühn, H.-J., Rehmer, B., Peter, F., Fedelich, B., Falkenberg, R., Haftaoglu, C., Kindrachuk, V., 2015. TMF-Lebensdauerberechnung ATL-Heißteile II - Erweiterung bestehender Werkstoff- und Rechenmodelle zur Lebensdauervorhersage für Abgasturbolader-Heißteile unter thermomechanischer Ermüdungsbeanspruchung. Final Report of the project Nr. 1100. Vol. 1082, Forschungsvereinigung Verbrennungskraftmaschinen e.V. (FVV), Frankfurt/Main, Germany.

Hawkyard, M., Powell, B. E., Hussey, I., Grabowski, L., 1996. Fatigue crack growth under the conjoint action of major and minor stress cycles. Fatigue Fract Eng Mat. Structures 19, 217-227.

Metzger, M.; Nieweg, B.; Schweizer, C.; Seifert, T., 2013. Lifetime prediction of cast iron materials under combined thermomechanical fatigue and high cycle fatigue loading using a mechanism-based model. International Journal of Fatigue 53, 58-66.

Moalla, M., Lang, K.-H., Löhe, D., 2001. Effect of superimposed high cycle fatigue loadings on the out-of-phase thermal-mechanical fatigue behaviour of CoCr22Ni22W14. Materials Science and Engineering A319–321, 647–651.

Nicholas, T., 2006. High Cycle Fatigue: A Mechanics of Materials Perspective. Elsevier, Amsterdam.

Riedel, H., 1987. Fracture at high temperature. Springer-Verlag, Berlin.

Shih, C. F., 1981. Relationships between the J-integral and the crack opening displacement for stationary and extending cracks. J Mech. Phys. Solids 29, 305-326.

Schweizer, C., Seifert, T., Nieweg, B., Von Hartrott, P., Riedel, H., 2011. Mechanisms and modelling of fatigue crack growth under combined low and high cycle fatigue loading. Int J Fatigue 33, 194-202.